

# Experimental and Computational Investigation of EVOH/Clay Nanocomposites

D. Aleperstein,<sup>1,2</sup> N. Artzi,<sup>1</sup> A. Siegmann,<sup>1,3</sup> M. Narkis<sup>1</sup>

<sup>1</sup>Department of Chemical Engineering, Technion, Israel Institute of Technology, Haifa 32000, Israel

<sup>2</sup>Department of Mechanical Engineering, Academic Braude College, Carmiel, Israel

<sup>3</sup>Department of Materials Engineering, Technion, IIT, Haifa 32000, Israel

Received 16 August 2003; accepted 20 October 2004

DOI 10.1002/app.21937

Published online in Wiley InterScience (www.interscience.wiley.com).

**ABSTRACT:** Ethylene–vinyl alcohol copolymer (EVOH)/organoclay nanocomposites were prepared via a dynamic melt-intercalation process. The effect of compatibilizers on the melt blending torque, intercalation level, and morphology of EVOH/organoclay systems was investigated. Maleic anhydride grafted ethylene vinyl acetate (EVA-g-MA), or maleic anhydride grafted linear low-density polyethylene (LLDPE-g-MA), were used to compatibilize EVOH with clay, at various concentrations (1, 5, and 10 wt %). Computer-simulation techniques are used to predict structural properties and interactions of EVOH with compatibilizers in the presence and absence of clay. The simulation results strongly support the experimental findings and their interpretation. X-ray diffraction shows enhanced intercalation within the galleries when the compatibilizers were added. Interestingly, results were obtained for the EVOH/clay/

compatibilizer systems, owing to a high level of interaction developed in these systems. Thermal analysis shows that, upon increasing the compatibilizer content, lower crystallinity levels result, until at a certain compatibilizer content no crystallization is taking place. Significantly higher mixing viscosity levels were obtained for the EVOH/organoclay blends compared with the neat EVOH polymer. The storage modulus was higher compared with the uncompatibilized EVOH/organoclay blend in the presence of EVA-g-MA compatibilizer (at all concentrations), and only at low contents of LLDPE-g-MA. © 2005 Wiley Periodicals, Inc. *J Appl Polym Sci* 97: 2060–2066, 2005

**Key words:** nanocomposites; EVOH; clay; compatibilizer; simulation

## INTRODUCTION

Polymer melt processing can be used to develop polymer–clay nanocomposites, using a conventional melt-mixing technology.<sup>1</sup> Polymer intercalation depends on the presence of specific interactions of the polymer chains with the organoclay. Pristine silicate layers of clay have polar hydroxyl groups and are thus incompatible with polyolefin. Hence, for example, polypropylene (PP)/organoclay nanocomposites are prepared by using a functional oligomer as compatibilizer, such as maleic anhydride modified PP oligomer.<sup>2</sup> Compatibilization is a common method to mediate an attractive interaction between phases, enhancing the formation of a desired morphology and the associated mechanical properties. In general, compatibilizers reduce interfacial tension leading to increased interphase adhesion, finely dispersed morphology, and stability against gross segregation.

The phenomenon of polymer chains confined in a nanoscale gap between rigid walls was previously investigated, both experimentally<sup>3,4</sup> and computation-

ally.<sup>5–7</sup> The main goal was to model and understand the confinement effect on the polymer entropy, as reflected by its configurational state. Monte Carlo and molecular dynamic computer simulations were used to explore the atomic scale structure and dynamics of intercalated polyethylene oxide (PEO)/montmorillonite nanocomposites.<sup>5</sup> The dynamics of confined polystyrene<sup>6</sup> or PEO chains<sup>7</sup> were studied.

A recent study of melt mixing of ethylene–vinyl alcohol copolymer (EVOH) with organoclay under dynamic conditions<sup>8</sup> has revealed that, despite the high interaction level between the polar EVOH and the organoclay, which has led to a mixed intercalation and delamination morphology, some mechanical properties were deteriorated. This was attributed mainly to a decline of EVOH crystallinity level, owing to interrupted crystallization caused by the high EVOH/clay interaction level. In addition, the low molecular weight onium ions treating the clay may locally plasticize the EVOH matrix when delamination occurs. In an attempt to improve the interaction level of the EVOH matrix with the clay tactoids, and simultaneously increase the level of intercalation and exfoliation, different compatibilizers were used.

This study focuses on the influence of compatibilizers (i.e., maleic anhydride grafted EVA, EVA-g-MA, or

Correspondence to: M. Narkis (narkis@txchnion.ac.il).

maleic anhydride-grafted LLDPE, LLDPE-g-MA) and processing conditions on the resulting EVOH/clay nanocomposite morphology, intercalation/exfoliation levels, and the thermal and dynamic mechanical behavior. The interaction of EVOH chains confined between nanometric montmorillonite clay galleries, with the clay itself, its surface modifiers, and compatibilizers, was studied experimentally and computationally. In this study, the enthalpic behavior, rather than the entropic one, is used to compare the experimental and the computational results.

## EXPERIMENTAL

### Materials

The EVOH used in this study is a commercial product containing 32 mol % ethylene, of Kuraray (Okayama, Japan). The treated clay used is Nanomer-1.30E clay, an onium ion modified montmorillonite mineral, obtained from Nanocor (IL). This organoclay contains 70–75 wt % montmorillonite and 25–30 wt % octadecylamine (ODA). It is claimed to be designed for ease of dispersion in amine-cured epoxy resins to form nanocomposites. The following two types of compatibilizers were studied: EVA-g-MA (trade name, Orevac, from Atofina, Paris, France) and LLDPE-g-MA from Mitsui (Tokyo, Japan). Both contain less than 2 wt % maleic anhydride (MA).

### Preparation methods

Prior to melt blending, the EVOH was ground into powder. The polymer and clay powders were dried in vacuum at 80 and 60°C, respectively, for 15 h. The components were dry-blended at selected ratios, and subsequently melt-mixed, in a Brabender plastograph machine, equipped with a 50-cm<sup>3</sup> cell, at 230°C and 60 rpm. The blends contained 15 wt % clay and different amounts (1, 5, 10 wt %) of EVA-g-MA or LLDPE-g-MA. An uncompatibilized 85/15 EVOH/clay sample was also prepared for comparison. All the resulting blends were compression molded at 230°C and 1000 MPa into 3-mm-thick plaques and subsequently characterized.

### Characterization

Differential scanning calorimetry (DSC) was employed to characterize the thermal behavior of the composites. A Mettler DSC 30 system, under nitrogen atmosphere, at a heating rate of 10°C/min was used. Samples were heated to a temperature above their melting, cooled at the same rate, and subsequently reheated. The melting behavior was determined from the second heating run. Dynamic mechanical properties of the compression-molded samples were measured by using a dynamic mechanical thermal analysis

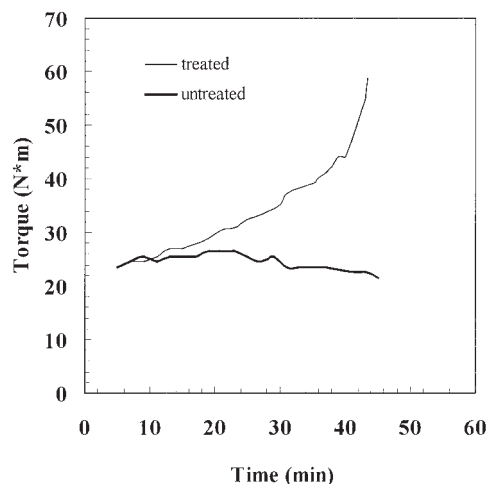


**Figure 1** Brabender plastogram of 85/15 EVOH/clay blends at 230°C and 60 rpm.

system (DMTA, Perkin–Elmer Series 7), in the three-point bending mode. The system was operated at 1 Hz, under nitrogen atmosphere, at a heating rate of 3°C/min. The structure of the composites was examined by a Philips X'PERT system X-ray diffraction (XRD), with a CuK $\alpha$  radiation source operated at 40 kV, 40 mA at a scanning rate of 0.5°/min. The blends' phase morphology was studied by using a JEOL JSM 5400 scanning electron microscope (SEM) to observe freeze-fractured and microtomed surfaces. All samples were gold sputtered prior to observation. The samples were further characterized by using a TA Thermogravimetric Analyzer (TGA) 2050, under air atmosphere, at a heating rate of 20°C/min. Simulations were done using Accelrys molecular modeling package Cerius2 and InsightII.<sup>9,10</sup> The montmorillonite simulation cells were constructed by the surface builder in Cerius2.<sup>9</sup> Energy minimization of all the different montmorillonite cells was carried out by using an Accelrys Universal force field.<sup>9</sup> The interaction between the EVOH polymer and LLDPE-g-MA and EVA-g-MA compatibilizers as well as the ODA surface treatment were examined by using InsightII<sup>10</sup> according to the following simulation sequence:

1. Amorphous cells of EVOH and ODA and/or LLDPE-g-MA and EVA-g-MA compatibilizers were constructed and energy was minimized by using the Amorphous Cell program<sup>10</sup> (10 samples of each kind).
2. The cells were subjected to molecular dynamics runs by using Discover program with COMPASS force field.<sup>10</sup> Each run consisted of 100,000 1-fs steps using the last 20,000 steps for data acquisition; each 500 steps for one conformation (frame), thus creating a 40-frame (conformations) trajectory each run. For the 10 samples, 400 different conformations were produced.

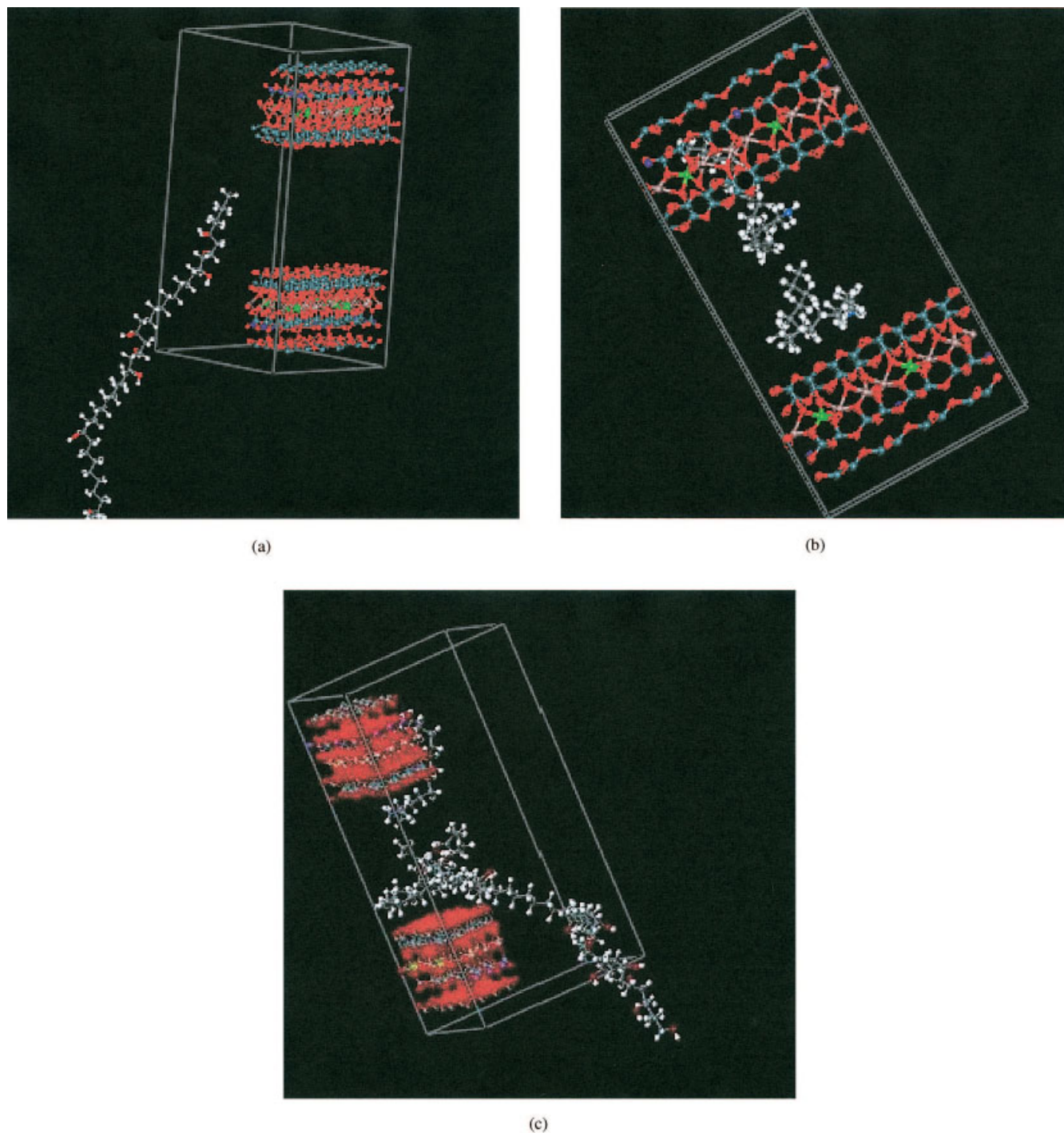


**Figure 2** An energy minimized simulation cell for (a) an untreated montmorillonite with EVOH chain; (b) octadecylamine-treated clay; (c) octadecylamine-treated clay with EVOH chain.

3. The interactions between the different functional groups were examined by using the pair correlation function in Amorphous Cell.<sup>10</sup> This function calculates the probability of finding two predefined functional groups in a certain distance from each other. If the distances between the two functional groups are evenly divided, the calculated function value is about a unit. A graph of

the calculated function value, namely, the intensity versus distance between the examined groups, shows a curve fluctuating around the value of a unit. If, however, the functional groups are not evenly divided (i.e., special interaction), then the pair correlation function graph shows an intensity peak at this specific distance with an intensity greater than 1, sometimes by a few



units. The intensity value indicates the interaction intensity and the width of the peak indicates the distance distribution of the functional groups. Hence, a large narrow peak implies a strong interaction.

## RESULTS AND DISCUSSION

### EVOH/clay system

Intercalation and/or delamination of clay in the presence of EVOH can be accomplished by melt-mixing in a Brabender Plastograph cell.<sup>11</sup> In a recent study, it was shown that during melt mixing the processing torque (viscosity) of the EVOH composite with untreated clay (85/15 EVOH/untreated clay) was practically constant, implying that the clay particles remain intact, behaving essentially as regular filler particles. However, the viscosity of the composite with treated clay (85/15 EVOH/treated clay) was rising due to clay fracturing processes, formation of new surfaces, and additional interaction with the EVOH matrix (Fig. 1). The energy-minimized simulation of untreated Na<sup>+</sup>/montmorillonite with a gallery gap of 16 Å with an EVOH chain is shown in Figure 2(a). It is seen that there is no thermodynamic drive for the EVOH chain to penetrate the clay gallery. The expected loss of conformational entropy is not compensated with sufficient interaction energy: thus, the polymer chain cannot intercalate into the clay gallery, in agreement with the experimental Brabender plastogram (Fig. 1). Figure 2(b) shows ODA-treated montmorillonite after energetic minimization (without EVOH). The amine group is located close to the clay gallery surface, while the aliphatic tail is directed away from the surface, due to the electrostatic interaction between the ammonium ion and the charged gallery surface. Figure 2(c) shows the same ODA-treated montmorillonite after energetic minimization in the presence of an EVOH chain. Contrary to the case presented in Figure 2(a), the loss of conformational entropy is now well compensated by interaction of the polymer chain with the surfactant (ODA). The polymer chain intercalates the galleries, causing gap widening, in agreement with the mixing viscosity increase shown in Figure 1. Moreover, as seen in Figure 2(c), the polymer has no contact with the clay surface but rather interacts mostly with the ODA surfactant. Hence, a mixture of EVOH and ODA should well simulate the polymer/surfactant interactions, and thus, indicate their intensity. The interaction between a hydroxyl group in EVOH and an amine group in ODA clay treatment is presented in Figure 3, showing its pair correlation function. Weak hydrogen bonding interaction centered on the distance of 2 Å is indicated, presumably accounting for the intercalation of EVOH into the clay galleries.

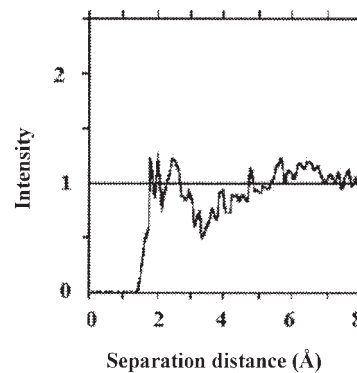


**Figure 3** Interaction intensity as a function of distance between an EVOH hydroxyl group and ODA amine.

### EVOH/compatibilizer/clay system

In a previous publication, an increased clay basal spacing in the presence of EVOH was shown, which further increases in compatibilized systems, and becomes more significant for higher compatibilizer contents.<sup>12</sup> The neat organoclay has a characteristic peak at  $2\theta = 3.58^\circ$  ( $d_{001} = 25$  Å) and by incorporation of 15 wt % clay into EVOH an intercalated structure with a gallery spacing of 32 Å ( $2\theta = 2.72^\circ$ ) results. Reference samples (without EVOH) of 85/15 EVA-g-MA/organoclay and 85/15 LLDPE-g-MA/organoclay were experimentally studied to characterize the tendency of each neat compatibilizer to intercalate, showing significant different gallery heights of 42 and 29 Å, respectively. EVOH/clay systems containing 1, 5, and 10 wt % EVA-g-MA exhibit characteristic peaks at 2.6, 2.5, and  $2.3^\circ$  ( $d_{001} = 33, 35, \text{ and } 38$  Å), respectively. The gallery heights of the corresponding blends containing LLDPE-g-MA are 34, 35, and 38 Å, respectively, same as obtained for the EVA-g-MA. Although EVA-g-MA itself tends to intercalate more than LLDPE-g-MA and more than EVOH, the final gallery heights for the EVOH/organoclay composites were similar for the two compatibilizers. Figure 4 shows the interaction of EVOH hydroxyl hydrogen with the grafted maleic anhydride etheric oxygen [Fig. 4(a)] or carbonyls [Fig. 4(b)]. The interaction with the carbonyl oxygens is significantly stronger than with the etheric oxygen (<2 Å versus 4 Å). The same trend is observed for EVA-g-MA interactions with EVOH. Figure 4(c) shows the interaction of EVOH hydroxyl hydrogen with the LLDPE-g-MA carbonyl oxygen in the presence of ODA (treated clay). The interaction intensity is enhanced compared to that without ODA [Fig. 4(b)], supporting the compatibilizer's effect in enhancing the interaction of EVOH and ODA in the treated clay. The EVOH interaction with the EVA-g-MA carbonyl oxygen is similar to the LLDPE-g-MA case, although the EVA-g-MA functions as a better compatibilizer, as evidenced by the higher interaction intensity, 4 versus 3

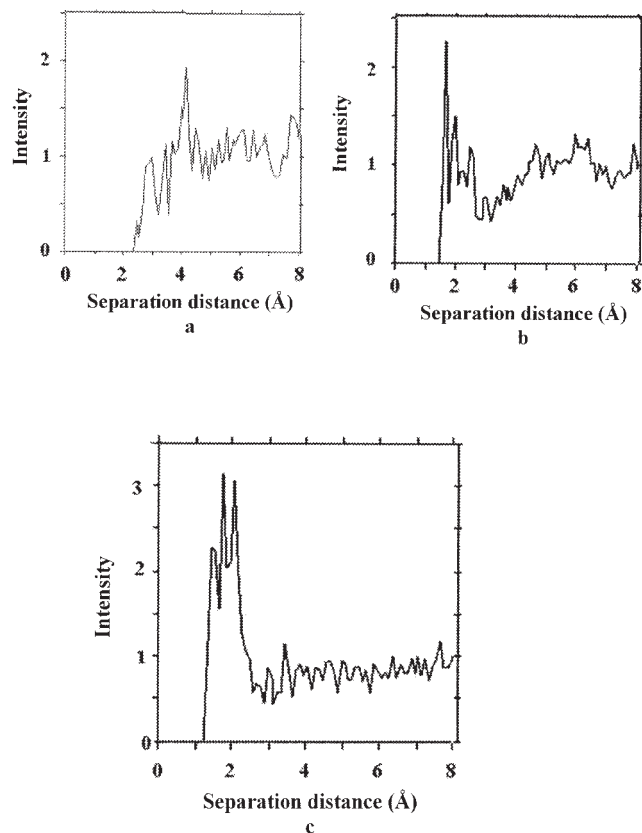


**Figure 4** EVOH interaction with LLDPE-g-MA: interaction intensity as a function of distance between the EVOH hydroxyl hydrogen and (a) maleic etheric oxygen; (b) maleic carbonyl; (c) maleic carbonyl groups in the presence of ODA.

(not shown). The nature of the interaction between the EVOH hydroxyl hydrogen and the maleic anhydride carbonyl oxygens grafted on the EVA is shown in Figure 5(a). Strong hydrogen bonds are shown with the carbonyl oxygens, one of 1.71 Å and the other of 1.83 Å. The hydrogen bond with the etheric oxygen is insignificant, having a bond length of 3.77 Å, as previously shown in Figure 4(a). The presence of ODA

enables the formation of additional hydrogen bonding between the amine hydrogen (in ODA) and EVOH hydroxyl oxygen [Fig. 5(b)]. This additional hydrogen bonding results in shorter hydrogen bond length between the EVOH hydroxyl hydrogen and the maleic carbonyl oxygen (1.79 Å instead of 1.83 Å). Thus, hydrogen bonding in the presence of ODA is intensified. The same trend was observed for EVOH with LLDPE-g-MA as a compatibilizer, in the presence of ODA (i.e., enhancement of hydrogen bonding), although at a longer bond length (1.93 Å), which supports the better compatibilizing performance of EVA-g-MA. This finding is consistent with SEM micrographs (Fig.6) showing the two compatibilizers in the EVOH matrix. The dispersed EVA-g-MA particles are significantly smaller than the LLDPE-g-MA ones, indicating a better compatibility of the former with EVOH. Figure 7 depicts room temperature microtomed surfaces of the [75/15/10 EVOH/clay/EVA-g-MA] and [75/15/10 EVOH/clay/LLDPE-g-MA] systems. Highly stretched fibrils crossing the cracks formed are seen in both systems. The observed voids may represent clay tactoids that have been pulled out by microtoming. The voids' size and thus the clay tactoids are larger in the case of LLDPE-g-MA [Fig. 7(b)] compared with EVA-g-MA [Fig. 7(a)], in agreement with micrographs of freeze-fractured surfaces (not shown here).

The effect of the compatibilizers on the dynamic mechanical properties of neat EVOH, in the absence of clay, was first studied.<sup>12</sup> The compatibilizers are expected to lower the modulus of the blends, owing to their lower modulus, a phenomenon which will be more pronounced for higher compatibilizer contents. Indeed, this process occurs in the case of LLDPE-g-MA. However, when EVA-g-MA is used, although the moduli decrease for EVA-g-MA contents higher than 1 wt %, the moduli are higher than that of the neat EVOH, for all studied EVA-g-MA contents. Moduli increase as a result of an addition of compatibilizer,

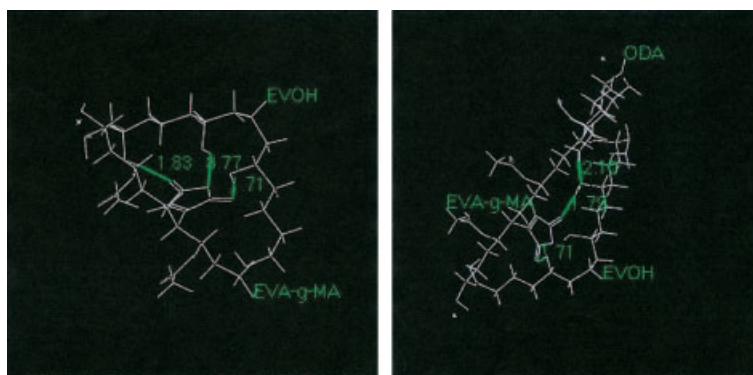


**Figure 5** Calculated spatial configuration of a single EVOH chain with EVA-g-MA: interaction of the EVOH hydroxyl hydrogen and the maleic carbonyl (a) no ODA, (b) with ODA.

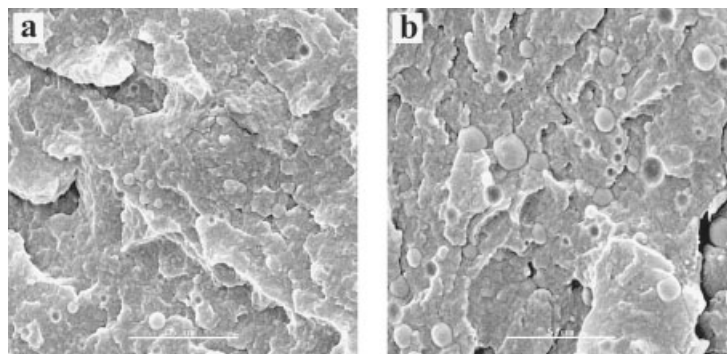


**Figure 6** SEM micrograph of (a) EVA-g-MA, (b)- LLDPE-g-MA in EVOH.

reminds the phenomenon seen when low contents of plasticizers are added to certain polymers and increase their modulus and tensile strength (i.e., act as antiplasticizers). The glassy storage modulus of EVOH containing 15 wt % clay is lower than that of the neat EVOH owing to crystallinity depression and plasticizing effect of the low molecular weight onium ions treating the clay. Upon EVA-g-MA addition at 1 and 5 wt % concentrations, the modulus increases; however, at 10 wt % EVA-g-MA, the modulus decreases and is even lower than that of the neat EVOH modulus. Incorporation of 1 wt % LLDPE-g-MA resulted in a slight modulus increase compared with the uncompatibilized blend containing 15 wt % clay; however, the modulus was lower than that of the neat EVOH polymer (not shown here). The fracturing/delamination processes are accompanied by an increased level of interaction in the studied systems, which results in two opposing effects on the storage modulus. The first, common in nanocomposites, is the modulus increase due to the increased polymer/clay interaction level. The second, unique to the presently studied EVOH matrix polymer, is a modulus decrease due to the crystallinity degree drop, ultimately even to its complete elimination (not shown here). In the EVOH/organoclay systems, the clay has a significant effect on crystallinity, whereas in EVOH/compatibilizer

pairs (without clay), no crystallinity change occurs. It is thus suggested that, by creation of additional clay surfaces, further reduction of crystallinity results. In this regard, LLDPE-g-MA is more aggressive than EVA-g-MA in reducing the degree of crystallinity in the EVOH/clay composites. This is because the latter is a better intercalant, and the former, therefore, located at a higher content in the matrix, is external to the clay particles. This is in agreement with the simulation results showing higher interaction level between EVOH and EVA-g-MA compared with LLDPE-g-MA. In addition, because LLDPE-g-MA interaction with clay is lower than EVA-g-MA's, more bare clay surfaces are available for interaction with EVOH. This clay/EVOH interaction is the one responsible for the reduction in the degree of crystallinity and thus on the resulting mechanical properties.

## CONCLUSIONS

Computer simulation is a useful tool to predict interactions of polymers with given clays or compatibilizers and thus enables the design of an efficient experimental program.

Dynamic melt-mixing of EVOH/organoclay mixtures is accompanied by a significant torque increase owing to clay particle fracturing, intercalation, and

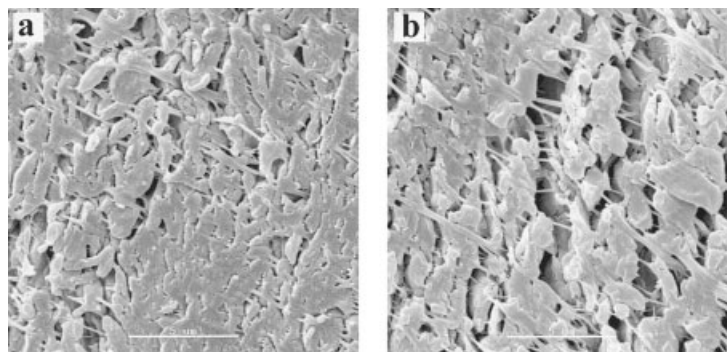


**Figure 7** SEM micrographs of microtomed surfaces of EVOH/clay/compatibilizer: (a) [75/15/10 EVOH/clay/EVA-g-MA], (b) [75/15/10 EVOH/clay/LLDPE-g-MA].

delamination processes and thus the build-up of significant levels of polymer/clay interaction.

The presence of compatibilizers enhances the intercalation level of EVOH into clay galleries. Nevertheless, the compatibilizer type, owing to different interaction levels with EVOH, affects the mechanical behavior of the composites, as found experimentally and supported by computer simulation.

## References

1. Vaia, R. A.; Ishii, H.; Giannelis, E. P. *Chem Mater* 1993, 5, 1694.
2. Hasegawa, N.; Kawasumi, M.; Kato, M.; Usuki, A.; Okada, A. *J Appl Polym Sci* 1996, 67, 87.
3. Anastasiadis, S. H.; Karatasos, K.; Vlachos, G.; Manias, E.; Giannelis, E. P. *Phys Rev Lett* 2000, 84, 915.
4. Manias, E.; Chen, H.; Krishnamoorti, R.; Genzer, J., Kramer, E. J.; Giannelis, E. P. *Macromolecules* 2000, 33, 7955.
5. Hackett, E.; Manias, E.; Giannelis, E. P. *Chem Mater* 2000, 12, 2161.
6. Manias, E.; Kuppaa, V. *Eur Phys J E* 2002, 8, 193.
7. Kuppaa, V.; Manias, E. *J Chem Phys* 2003, 118, 3421.
8. Artzi, N.; Nir, Y.; Narkis, M.; Siegmman, A. *J Polym Sci, Part B: Polym Phys* 2002, 40, 1741.
9. Cerius2 manual; Accelrys: San Diego, 2001.
10. Material Studio manual; Accelrys: San Diego, 2002.
11. Artzi, N.; Nir, Y.; Wang, D.; Narkis, M.; Siegmman, A. *Polym Comp* 2001, 22, 710.
12. Artzi, N.; Nir, Y.; Narkis, M.; Siegmman, A. *Polym Comp* 2003, 24, 627.